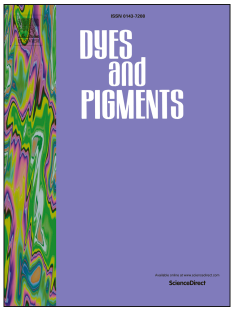

Characteristic absorption band split of symmetrically tetra-octyloxy metal phthalocyanines

Fangdi Cong, Zhen Wei, Zhiqiang Huang, Fengyang Yu, Haixue Liu, Jing Cui, Helong Yu, Xinxin Chu, Xiguang Du, Kezhi Xing, Jianhong Lai

PII: S0143-7208(15)00109-6
DOI: 10.1016/j.dyepig.2015.03.034
Reference: DYPI 4715

To appear in: *Dyes and Pigments*

Received Date: 17 January 2015
Revised Date: 22 March 2015
Accepted Date: 26 March 2015

Please cite this article as: Cong F, Wei Z, Huang Z, Yu F, Liu H, Cui J, Yu H, Chu X, Du X, Xing K, Lai J, Characteristic absorption band split of symmetrically tetra-octyloxy metal phthalocyanines, *Dyes and Pigments* (2015), doi: 10.1016/j.dyepig.2015.03.034.

Characteristic absorption band split of symmetrically tetra-octyloxy metal phthalocyanines

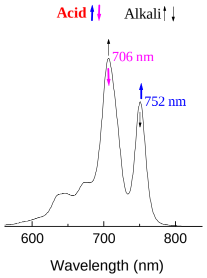

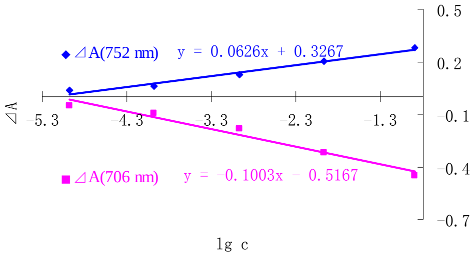

Characteristic absorption band split of symmetrically tetra-octyloxy metal phthalocyanines

Fangdi Cong[1] *, Zhen Wei[1], Zhiqiang Huang[1], Fengyang Yu[1], Haixue Liu[1], Jing Cui[1], Helong Yu[2], Xinxin Chu[2], Xiguang Du[2] **, Kezhi Xing[1] **, Jianhong Lai

[1]Tianjin Key Laboratory of Aqua-ecology and Aquaculture, College of Basic Science, Tianjin Agricultural University, Tianjin 300384, P.R. China;

[2]Faculty of Chemistry, Northeast Normal University, Changchun 130024, P.R. China

*Address of the first author and the corresponding author: (Fangdi Cong) Jinjing Road, No. 22, Tianjin 300384, China, congfangdi@163.com;

**Address of the co-corresponding authors: (Xiguang Du) Renmin Road, No. 5268, Changchun 130024, china, email: xgdunenu@163.com; (Kezhi Xing) Jinjing Road, No. 22, Tianjin 300384, China, email: xingkezhitn@163.com.

Abstract: An interesting phenomenon was that some symmetrically substituted metal phthalocyanines behaved characteristic absorption band split in non-coordinated solvents especially when they had zinc as the center metal and alkyloxy substituted groups at non-periphery of molecular skeleton, for example tetra-α-octyloxy zinc phthalocyanine having split peaks at 706 and 752 nm in chloroform, respectively. The red split peak at 752 nm could be strengthened by acid enhancing macromolecular conjugation, and contrarily weakened by alkali. Further a linear relationship was found between the relatively alteration value of characteristic absorbance and the concentration logarithm of acid in chloroform from 1.18 $\times 10^{-5}$ to 1.39$\times 10^{-1}$ mol/L, which implied its potential application in analysis on trace of total acids included in grain, food and medicine, etc.

Keywords: Q band split; monoprotonation; J-dimer; phthalocyanine; conjugation

1 Introduction

Phthalocyanine (Pc) macromolecules have significant applications in high technology fields such as catalysis, electrochromic devices, gas sensor, non-linear optical, photodynamic therapy and photovoltaic cell, etc., for the unique 18-electron π planar conjugate system of them [1]. The structure endows them with characteristic absorptions around 700 nm, namely called Q band, which can be tuned by changing the center metal, substituent, substituted position (peripherally, β or non-peripherally, α), linker heteroatom (oxygen, sulfur or nitrogen) at Pc skeleton, molecular symmetry, intermolecular aggregation and solvents [2]. Generally, the Q band appears in a single peak for symmetric Pcs, e.g., tetra or octo-substituted metal Pcs, and in two split peaks for metal-free, unsymmetric or some aggregated metal Pcs [3,4]. An exception is that a few symmetrically substituted metal Pcs, especially tetra-α-alkoxy-substituted zinc Pc, exhibit two Q band split peaks instead of one normal single peak in non-coordinated solvents, e.g., chloroform, dichloromethane and benzene [5-9]. Clarifying the Q band split of symmetrically substituted metal Pcs is very critical for researchers to find novel molecular information, or design new Pc molecules with desired photophysical and photochemical properties [10,11]. The split has ever been argued to be derived from intermolecular J-dimers (aggregate of two molecules in side-to-side form) or monoprotonation of aza-nitrogen atom in Pc skeleton, but the opinions fail to agree and the related study on split peak profile, split range and chemical characterization is still inadequate [12]. Thus tetra-α-octyloxy substituted zinc Pc (αOZnP), tetra-β-octyloxy substituted zinc Pc (βOZnP) and tetra-α-octyloxy substituted copper Pc (αOCuP) (Scheme 1) are synthesized and studied in this paper.

2 Experimental

2.1 Materials and methods

DMSO was pre-dried over BaO and distilled under reduced pressure. Column chromatography purifications were preformed on silica gel. All other reagents and solvents are commercial available and used without further purification.

High-resolution ^{1}H NMR spectra were recorded on a Varian Unity 500 spectrometer. IR spectra were measured on a Shimadzu IRAffinity-1 spectrometer. UV-vis spectra were taken on a Shimadzu UV-visible-1800 spectrophotometer. MS spectra were obtained on a Voyager-De STR MALDI-TOF-MS spectrometer. Elemental analyses were performed on a PerkinElmer 2400 Elemental Analyzer.

2.2 Synthesis of 3- and 4-octyloxy-phthalonitriles

3-Nitrophthalonitrile **1** (6.92 g, 40 mmol) and n-octanol (7.5 mL, 48 mmol) were added to 60 mL anhydrous DMSO at RT. The reaction mixture was stirred and $LiOH \cdot H_2O$ (4.2 g, 100 mmol) was interfused over a 2-h period and the mixture was then stirred for 1 day. Reaction was monitored by TLC analysis. Then the reaction mixture was poured into 10% NaCl solution (400 mL) and stirred till precipitate appeared. The reaction product was collected by vacuum filtration. The crude product was purified by flash column chromatography with chloroform as the mobile phase to afford white power 3-octyloxy-phthalonitrile **3**: 8.4 g, yield: 82 %; ^{1}H NMR (500 MHz, $CDCl_3$): δ 7.70 (dd, 1H, ArH), 7.24 (d, 1H, ArH), 7.15 (d, 1H, ArH), 4.47 (m, 2H, OCH_2), 1.73 (m, 2H, CH_2), 1.27-1.34 (m, 8H, $(CH_2)_4$), 0.88 (m, 3H, CH_3); MS ($CHCl_3$): *m/z* calcd for [M + Na^+]: 279.3, found: 279.6 (an isotopic cluster peak) [M + Na^+]; IR (KBr, ν_{max}, cm^{-1}): 2231 ν_s (C=N), 1253 ν_s (C-O-C); Anal. Calcd for $C_{16}H_{12}N_2O$ (256.3): C 74.97, H 7.86, N 10.93, Found: C 74.93, H 7.63, N 10.85.

If the aforesaid synthesis began from 4-Nitrophthalonitrile **2**, the reaction mixture after reaction for 24 h was poured into 10% NaCl solution (400 mL) and the reaction product was collected by extraction with 100 mL chloroform twice. The combined organic layer was washed by 100 mL water and dried with Na_2SO_4. The crude product was collected by removing solvent and further purified by flash column chromatography with chloroform as the mobile phase to afford light yellow and sticky liquid 4-octyloxy-phthalonitrile **4**: 8.1 g, yield: 79 %; ^1H NMR (500 MHz, $CDCl_3$): δ 7.69 (d, 1H, ArH), 7.22 (s, 1H, ArH), 7.14 (d, 1H, ArH), 4.45 (m, 1H, OCH), 1.75 (m, 2H, CH_2), 1.28-1.35 (m, 8H, $(CH_2)_4$), 0.88 (m, 3H, CH_3); MS ($CHCl_3$): *m/z* calcd for [M + Na^+]: 279.3, found: 279.4 (an isotopic cluster peak) [M + Na^+]; IR (KBr, ν_{max}, cm^{-1}): 2234 ν_s (C=N), 1252 ν_s (C-O-C); Anal. Calcd for $C_{16}H_{12}N_2O$ (256.3): C 74.97, H 7.86, N 10.93, Found: C 74.85, H 7.67, N 10.97.

2.3 Synthesis of αOZnP and αOCuP

3-Octyloxy-phthalonitrile **3** (4.10 g, 16.0 mmol) was mixed with $Zn(AcO)_2 \cdot 2H_2O$ (0.88 g, 4.0 mmol), urea (10 g) and $(NH_4)_2MoO_4$ (0.05 g), and added in a 100 mL breaker. The breaker was covered with a watch glass and heated at 160℃ for 3 h in heat-collection-type heater (DF-101S). After cooling, the resultant green solid was ground and then washed with methanol by Soxhlet extraction to remove part of remnants. The collected solid was further purified by flash column chromatography with hexane and THF (3:2, v:v) as the mobile phase to give pure blue-green solid αOZnP: 2.8 g, Yield: 65 %; ^1H NMR (500 MHz, $CDCl_3$): δ 8.72-6.58 (m, broad, 12H, ArH), 4.60-3.91 (m, broad, 8H, $4OCH_2$), 2.42-1.25 (m, broad, 48H, $4(CH_2)_6$); 0.97 (t, 12H, $4CH_3$); MS ($CHCl_3$): *m/z* calcd for [M]: 1090.8, found: 1089.8 [M]; IR (KBr, ν_{max}, cm^{-1}): 1239 ν_s (C-O-C); Anal. Calcd for $C_{64}H_{80}N_8O_4Zn$: C, 70.47; H, 7.39; N, 10.27, Found: C 70.62, H 7.43, N 10.15.

Replacing $Zn(AcO)_2 \cdot 2H_2O$ (0.88 g, 4.0 mmol) with $CuCl_2 \cdot 2H_2O$ (0.68 g, 4.0 mmol) in the aforesaid performance, the final product was blue solid αOCuP: 3.9 g, Yield: 89 %; ^1H NMR (500 MHz, $CDCl_3$): δ 10.61-8.16 (s, weak and broad, 12H, ArH), 4.54-3.53 (d, weak and broad, 8H, $4OCH_2$), 2.25-1.22 (q, broad, 48H, $4(CH_2)_6$); 0.94 (s, broad, 12H, $4CH_3$); MS ($CHCl_3$): *m/z* calcd for [M]: 1087.6, found: 1088.8 [M]; IR (KBr, ν_{max}, cm^{-1}): 1233 ν_s (C-O-C); Anal. Calcd for $C_{64}H_{80}N_8O_4Cu$: C, 70.59; H, 7.41; Cu, 5.84; N, 10.29, Found: C 70.33, H 7.48, N 10.46.

2.4 Synthesis of βOZnP

4-Octyloxy-phthalonitrile **4** (4.10 g, 16.0 mmol) was mixed with $Zn(AcO)_2 \cdot 2H_2O$ (0.88 g, 4.0 mmol), urea (10 g) and $(NH_4)_2MoO_4$ (0.05 g), and added in a 100 mL breaker. The breaker was covered with a watch glass and heated at 160℃ for 3 h in heat-collection-type heater (DF-101S). After cooling, the resultant green solid was ground and then washed with methanol by Soxhlet extraction to remove part of remnants. In the end, the collected solid was purified by flash column chromatography with hexane and THF (3:2, v:v) as the mobile phase to give pure blue-green solid βOZnP: 2.2 g, Yield: 51 %; ^1H NMR (500 MHz, $CDCl_3$): δ 7.57-6.16 (m, broad, 12H, ArH), 4.03-3.46 (d, broad, 8H, $4OCH_2$), 1.79-1.24 (m, broad, 48H, $4(CH_2)_6$); 1.04 (t, 12H, $4CH_3$); MS ($CHCl_3$): *m/z* calcd for [M]: 1090.8, found: 1089.7 [M]; IR (KBr, ν_{max}, cm^{-1}): 1238 ν_s (C-O-C); Anal. Calcd for $C_{64}H_{80}N_8O_4Zn$: C, 70.47; H, 7.39; N, 10.27, Found: C 70.55, H 7.17, N 10.43.

2.5 Spectral analysis

The solution of synthesized Pc compounds were prepared by way of calculation, weighting, dissolution and dilution, and the detected solution added in cuvette for UV-vis analysis was unified in the volume of 3 mL. Acid (alkali) was first dissolved in solvent to obtain 100000 ppm solution and then diluted into 10000, 1000, 100, 10, 1 ppm, and so on. Effect of acid (alkali) on Pc spectra was processed by adding a drop of acid (alkali) solution in accordance with the concentration order from low to high into the cuvette with 3 mL Pc solution, and mixed and detected. The actual molar concentration of acid (alkali) in the detected Pc solution was calculated based on ppm concentration of acid (alkali), solution mass of a drop of acid (alkali), and volume of detected Pc solution.

3 Results and discussion

3.1 Q band split and J-dimer

J-dimers were aggregates constructed by two Pc molecules in side-to-side form, which caused molecular symmetry down from monomolecular D_{2h} to J-dimer C_{2v} point group and thus led to Q band split [1]. The theoretical computations also showed that it was favorable for zinc Pc to aggregate in form of dimers, trimers and oligomers [13], especially when structurally suitable substituents linked with Pc ring or felicitously axial ligands existed [2,14]. But the reported Pc J-dimers were less, and few of them were actually obtained and successfully characterized [2]. As far as we knew, the rigid Pc J-dimer could be synthesized only by careful work [15], and non-rigid Pc J-dimers were formed only by coordination between the center metal and the fit substitution atom of two unsymmetrical Pcs [16,17], or by intermolecular interaction between two symmetrically substituted metal Pcs with their substituents included in size-suitable cyclodextrins [18].

In most cases, those symmetrically substituted metal Pcs behaving Q band splits in non-coordinated solvents were concluded to be assembled into J-dimers by coordination between the center metal and the linker atom such as oxygen, sulfur and nitrogen [19-31]. However, they were not fully proven, i.e., it was very insufficient in credible characterizations, e.g. MS and ^{1}H NMR [19-24], or out of proportion for the weak dimer MS speaks to the strong Q absorption band split peaks [25-31]. Fig. 2a showed that in chloroform symmetrically substituted αOZnP appeared two Q band split peaks: left blue peak (Q_L) at 706 nm and right red peak (Q_R) at 752 nm, which were ever deduced to be originated from J-dimer according to the previous conclusion [30,31]. But TOF-MS of αOZnP showed that only monomer peak was obvious and no dimer peak, even a very weak one as presented by tetra-α-aryloxy substituted zinc Pc [31], could be distinguished (Fig. 1). In addition, the other possible aggregate of αOZnP molecules in chloroform also could be ignored for that there were not two kinds of aggregation phenomena, occurring obvious change in the molar extinction coefficients of Q_L and Q_R, and appearing the inflexion point between them along with concentration alteration (Fig. 2a) [5,11]. All of these showed that here the Q band split of αOZnP in chloroform was not derived from J-dimers.

3.2 Q band split and protonation

Protonation on aza-nitrogen of Pc ring is an intensively discussed factor leading to Q band split [11]. As we all know, the aza-nitrogen of Pc molecule has alkalinity weaker than those of small aromatic amines, e.g., pridine and pyrrole, for the stronger p-π conjugation between aza-nitrogen and Pc ring. So the protonation of four aza-nitrogen atoms in Pc skeleton was weak and not same, and the first protonation could be realized by adding acid gradually but the second, third and fourth protonations were actually hard even if more much protonation reagent imported [32]. So the aforesaid

Q band split most likely resulted from the monoprotonation of αOZnP for existence of trace amount of acid from cleavage of chloroform [11]. Experimental displayed that αOZnP molecules were sensitive to acetic acid from 1.06×10^{-7} to 1.39×10^{-1} mol/L in which Q_L decreased and shifted red from 706 to 717 nm, and Q_R increased but did not obviously shift red (Fig. 2b). Comparatively, βOZnP had no Q band split appearance in chloroform, and appeared two split peaks till enough acetic acid mixed into solution but they were broad (Fig. 2c). Contrarily, adding triethylamine into solution of αOZnP in chloroform caused Q_R peaks to attenuate and disappear while Q_L rise and become the normal Q band in the end (Fig. 2d). All this showed that Q_R was a new peak generated from protonation of acid on aza-nitrogen atom in Pc skeleton [6,7]. The protonation also could be reflected by attenuation of shoulder peaks at 632 nm for αOZnP and 615 nm for βOZnP along with acid infused in solution of them in chloroform (Fig. 2b, c). Because shoulder peaks derived from n-π^* transition of lone pair electron in sp^2 orbit of aza-nitrogen atom [19,33-37], and protonation inevitably restricted the n-π^* transition and weakened the shoulder peak absorption. Provided that no aza-nitrogen atoms in conjugate macromolecules as porphyrin compounds, then no typical shoulder absorptions appeared [38,39].

3.3 Protonation and conjugation

The traditional explanation on Q band split induced by proton was attributed to the decrease in symmetry of Pc molecules for monoprotonation of aza-nitrogen atom [32]. The investigations showed that low symmetric Pc molecules seldom had a Q band split range more than 35 nm [1,9,40], and indeed a few of them had no Q band split observed for spectral overlap [40]. But symmetrically substituted metal Pc molecules unexpectedly had an about 45 nm of Q band split range in non-coordinated solvents in existence of protonation reagents [6,11,32,41], for instance *α*OZnP having a 46 nm of Q band split range in chloroform (Fig. 2a). Therefore there must be the other proton-induced effect to devote the so large Q band split to *α*OZnP. It was thought that protonation on aza-nitrogen atom obstructed *n*-*π** transition of lone pair electrons in sp^2 orbit and accordingly benefit the large *π* planar conjugation over Pc ring. The enhanced conjugation inevitably decreased HOMO-LUMO energy gap and then brought monoprotonated Pc with a shift-red Q_R relative to Q_L of unprotonated Pc, for enlarged conjugate structure and enhanced conjugation of Pc compounds generally leading to Q band shift red largely [5,42-45]. In terms of *α*OZnP, the linker oxygen atom is fixed by proton in nearby aza-nitrogen atom when protonation reagent existed for the advantage in steric hindrance (Fig. 3). The constraint on linker oxygen atom is similar to the hydrogen bond interaction in tetra-*α*-amino-substituted zinc Pc [46], which did not allowed *α*-octyloxyl group freely rotate around C-O bond linking octyloxy group to Pc ring and ensured *p*-*π* conjugation between linker oxygen and Pc ring more available to reinforce donation of lone pair electrons from oxygen through Pc ring to the center zinc. The result was that an electron-transferring absorption band at 418 nm, commonly appeared at the range from 400 to 500 nm [5,47], was observed and obviously elevated with increase of acetic acid (Fig. 2b). The effective *p*-*π* conjugation might cause the synergistic effect of another three linker oxygen atoms more effectively conjugating with Pc ring via delocalization of electron over Pc ring, as a result emerging a new molecular form $(\alpha\text{OZnP})H^+$ due to monoprotonation. In chloroform, *α*OZnP could be tuned to green monoprotonated $(\alpha\text{OZnP})H^+$ by enough acetic acid ($\geq 2.68\times10^{-1}$ mol/L) and blue proton-free *α*OZnP by little triethylamine ($\geq 6.59\times10^{-3}$ mol/L), exhibiting characteristic absorptions Q_R and Q_L, respectively (Fig. 2b, d and Fig. 3). The absorption at 717 nm was vested in *n*-*π** transition of unprotonated aza-nitrogen atoms in skeleton of (αOZnP)H$^+$ after acetic acid exceeding 2.54×10^{-1} mol/L and deemed as the shoulder peak of (αOPZ)H$^+$ (Fig. 2b). Differently, βOZnP molecules have no stable monoprotonated form in chloroform for the disadvantage of in steric hindrance and synergistic conjugation as in αOZnP. So βOZnP had no Q band split in chloroform until enough acid imported (Fig. 2c). Similar differences in Q band split were also met in some reported α- and β-substituted metal Pcs but lacking necessary interpretation [5,40,41,48].

3.4 Effect of solvents on Q band

In benzene (Fig. 4a), αOZnP had a Q split profile as presented in chloroform with acetic acid at 2.54 ≥ 10^{-1} mol/L, which implied that αOZnP was more inclined to form (αOZnP)H$^+$ in benzene than in chloroform. The reason might be that the conjugate effect over Pc was further strengthened by the conjugate effect from solvent benzene [49] besides protonation from trace of proton-donated compounds [11]. The spectra of αOZnP in benzene were not changed obviously by acid but could be tuned greatly by alkali decreasing Q_R at 752 nm, and increasing and shifting the overlap absorption from 717 to 697 nm. When triethylamine achieved at 6.59×10^{-3} mol/L, Q_R disappeared completely and Q_L at 697 nm divorced thoroughly from overlap with shoulder peak of (αOZnP)H$^+$ at 717 nm. Also the shoulder peak of αOZnP at 628 nm was recovered for deprotonation of aza-nitrogen by alkali. βOZnP has a spectral absorption in benzene similar to in chloroform with 3 droplets of acetic acid (Fig. 2c), which also could not be altered by adding acid but could be transformed into normal Q absorption by adding little alkali.

In THF (Fig. 4b), αOZnP had no Q band split and displayed a normal Q band at 699 nm and a shoulder peak at 628 nm due to deprotonation of oxygen atom in THF molecule [50]. But the spectra began to change obviously when adding more than two droplets of acetic acid in tested solution. More acid caused Q band, shoulder peak and B band gradually decrease and synchronously spawned a new peak at 749 nm as well as a band at 417 nm. They were assigned as Q_R and electron-transferring absorption of (αOZnP)H^+, respectively. When 20-30 droplets of acid were added in, Q_L and Q_R had similar profiles of αOZnP in chloroform. More than 30 droplets of acid caused the shoulder peak of (αOZnP)H^+ revealing at 715 nm, which was indistinguishable for spectral overlap with Q_L when acid insufficient. But more than 50 droplets of acid could not extinguish the peak Q_L at 699 nm or brought spectra with further remarkable changes for coordination and deprotonation of solvent THF. βOZnP was not impacted by acid and always gave normal spectra in THF.

3.5 Significance of the center metal

Symmetrically substituted zinc Pcs more easily displayed Q band splits for zinc d^{10} state and favorable planar conjugation structure based on already existing experimental data [3,51] and theoretical calculation [13]. Comparing αOCuP with αOZnP, the only difference lied in the center metal but αOCuP had no split Q_R peak besides normal Q (Q_L) band at 708 nm in chloroform (Fig. 5a). Adding acetic acid only brought αOCuP with weak absorption at 767 nm meant Q_R (Fig. 5a) and adding triethylamine gave no impact on its spectrum. In benzene, αOCuP had small Q_R absorption at 761 nm for extra conjugate effect of solvent benzene relative to chloroform [49]. Similarly, adding acetic acid brought it with no large change at 761 nm (Fig. 5b) and adding little triethylamine easily distinguished Q_R and left αOCuP with normal Q band. In THF, αOCuP had a normal Q band without impact from acid or alkali. This showed that αOCuP could not be easily protonated by acid, namely the alkalinity of aza-nitrogen atom in *α*OCuP was weaker than in *α*OZnP. That is to say that *p*-*π* conjugation in-between linker oxygen atom and Pc ring of *α*OCuP was very weak and then the large *π* planar conjugation could not be strengthened availably. So no electron-transferring absorption and distinct Q_R peak of *α*OCuP were observed in non-coordinated solvents (Fig. 5).

3.6 Tuning Q band split peaks by acid

The phenomena that trace of acid, e.g. at 1.06×10^{-7} mol/L (Fig. 2b), increasing Q_R and decreasing Q_L of *α*OZnP indicated that the inherent acid in chloroform was lower than 1.06×10^{-7} mol/L. In contrast, the relatively more alkali achieving at 6.53×10^{-4} mol/L was not enough to completely eliminate the Q_R peak in chloroform (Fig. 2d). Moreover even in coordinated solvent, e.g. THF, Q_R still could be evoked when enough acetic acid was imported (Fig. 4b). All these displayed that *α*OZnP was extremely sensitive to acid, especially in chloroform. Namely, *α*OZnP could be easily transferred into (*α*OZnP)H^+ through synergistic conjugate effect induced by protonation of protonated reagent due to the favorable structure in *α*OZnP (Fig. 3). If taking the solution of *α*OZnP in chloroform as a reference sample, the effect of acid on *α*OZnP was more clearly cognized on UV-vis spectrometer. Fig. 6a showed that the Q_R increased and inversely Q_L decreased gradually with more acid mixed in the solution of *α*OZnP in chloroform. The large variation of Q_R and Q_L was given by acetic acid with a concentration range from 1.18×10^{-5} to 1.39×10^{-1} mol/L in which a linear relationship was found between the relatively alteration value of characteristic absorbance in Q_R or Q_L ($\triangle A$) and the concentration logarithm of acetic acid (lg *c*) (Fig. 6b). It was imagined that the linearity would endowed *α*OZnP with an important application in the facile analysis on trace of total acid included in grain, food and medicine, etc.

Conclusions

Q band split of symmetrically substituted metal Pcs could be tuned by the center metal, substituted position, solvent, acid and alkali. *α*OZnP was inclined to generate Q band split in non-coordinated solvent for that the center zinc benefited planarization and conjugation of Pc ring, and *α*-substituted oxygen atom strengthened conjugation of Pc plane via synergistic *p*-*π* conjugation constructed by proton fastening the substituted oxygen with the aza-nitogen atom in Pc skeleton. Then there were two kinds of molecular forms *α*OZnP and (*α*OZnP)H^+ in chloroform, which were corresponding to Q split peaks Q_L and Q_R, respectively. Q_L and Q_R of *α*OZnP could be tuned by acid and alkali in whether coordinated or non-coordinated solvents. Moreover, a linear relationship was found between the relatively alteration value of characteristic absorbance in Q_R or Q_L (⊿A) and the concentration logarithm of acetic acid in chloroform (lg *c*) from 1.18×10^{-5} to 1.39×10^{-1} mol/L. The linearity might find application of *α*OZnP in the facile analysis on trace of total acid included in grain, food and medicine, etc. Nonetheless, the theoretically chemical calculation on *α*OZnP and (*α*OZnP)H^+ is still needed to be processed in the future.

Acknowledgment

The authors thank the National Natural Science Foundation of China (20540115) and the 41st Postdoctoral Science Foundation of China (20070410332), for financial support.

References

[1] Mack J, Kobayashi N. Low symmetry phthalocyanines and their analogues. Chem Rev 2011;111:281–321.

[2] Würthner F, Kaiser TE, Saha-Möller CR. J-Aggregates: from serendipitous discovery to supramolecular engineering of functional dye materials. Angew Chem Int Ed 2011;50:3376– 3410.

[3] Kobayashi N. Dimers, trimers and oligomers of phthalocyanines and related compounds, Coord Chem Rev 2002;227:129-152.

[4] Singh VK, Kanaparthi RK, Giribabu L. Emerging molecular design strategies of unsymmetrical phthalocyanines for dye-sensitized solar cell applications. RSC Adv 2014;4:6970–6984.

[5] Özçeşmeci I, Tekinb A, Gül A. Synthesis and aggregation behavior of zinc phthalocyanines substituted with bulky naphthoxy and phenylazonaphthoxy groups:An experimental and theoretical study. Synth Met 2014;189:100–110.

[6] Durmus M, Nyokong T. Synthesis and solvent effects on the electronic absorption and fluorescence spectral properties of substituted zinc phthalocyanines Polyhedron. Polyhedron 2007;26:2767–2776.

[7] Honda T, Kojima T, Kobayashi N, Fukuzumi S. Crystal structures and electronic properties of saddle-distorted and protonated phthalocyanines. Angew Chem Int Ed 2011;50:2725–2728.

[8] Chen Z, Zhong C, Zhang Z, Li Z, Niu L, Bin Y, Zhang F. Photoresponsive J-aggregation behavior of a Novel azobenzene-phthalocyanine dyad and its third-order optical nonlinearity. J Phys Chem B 2008;112:7387–7394.

[9] Huang X, Zhao F, Li Z, Tang Y, Zhang F, Tung C. Self-assembled nanowire networks of aryloxy zinc phthalocyanines based on Zn-O coordination. Langmuir 2007;23:5167-5172.

[10] Löslein H, Ameri T, Matt GJ, Koppe M, Egelhaaf HJ, Troeger A, Sgobba V, Guldi DM, Brabe CJ. Transient absorption spectroscopy studies on polythiophene–fullerene bulk heterojunction organic blend films sensitized with a low-bandgap polymer, macromol. Rapid Commun 2013;34:1090–1097.

[11] Ayhan MM, Özpınar GA, Durmuşa M, Gürek AG. Effects of position (*α* or *β*) and linker heteroatom (O or S) of substituent on the photophysicochemical behavior of poly(oxyethylene) substituted ZnPcs and assessment of J-aggregation or protonation using TD-DFT computations. Dalton Trans 2013;42:14892–14904.

[12] Ashokkumar R, Kathiravan A, Ramamurthy P. Aggregation behaviour and electron injection/ recombination dynamics of symmetrical and unsymmetrical Zn-phthalocyanines on TiO2 film. Phys Chem Chem Phys 2014;16:1015—1021.

[13] Ueno LT, Machado AEH, Machado FBC. Theoretical studies of zinc phthalocyanine monomer, dimer and trimer forms. J Mol Struct Theochem 2009;899:71-78.

[14] Yanagisawa S, Yasuda T, Inagaki K, Morikawa Y, Manseki K, Yanagida S. Intermolecular interaction as the origin of red shifts in absorption spectra of Zinc-phthalocyanine from first-principles. J Phys Chem A 2013;117:11246−11253.

[15] Asano Y., Muranaka A., Fukasawa A., Hatano T., Uchiyama M., Kobayashi N., anti-[2.2](1,4)Phthalocyaninophane: spectroscopic evidence for transannular interaction in the excited states. J Am Chem Soc 2007;129:4516-4517.

[16] Kameyama K, Morisue M, Satake A, Kobuke Y. Highly fluorescent self-coordinated phthalocyanine dimmers. Angew Chem Int Ed 2005;44:4763–4766.

[17] Tolbin AY, Pushkarev VE, Balashova IO, Tomilova LG. Synthesis of a stable J-type dimer based on the 2-hydroxy-9(10),16(17),23(24)-tri(tert-butyl)phthalocyanine zinc complex. Mendeleev Commun 2013;23:137-139.

[18] Morisue M, Ueda S, Kurasawa M, Naito M, Kuroda Y. Highly fluorescent slipped-cofacial phthalocyanine dimer as a shallow inclusion complex with α-cyclodextrin. J Phys Chem A 2012;116:5139-5144.

[19] Yi J, Chen Z, Xiang J, Zhang F. Photocontrollable J-aggregation of a diarylethene_phthalocyanine hybrid and its aggregation-stabilized photochromic behavior. Langmuir 2011;27:8061–8066.

[20] Gunsel A, Yarasir MN, Kandaz M, Koca A. Synthesis, H- or J-type aggregations, electrochemistry and in situ spectroelectrochemistry of metal ion sensing lead(II) phthalocyanines. Polyhedron 2010;29:3394-3404.

[21] Ogunsipe A, Maree D, Nyokong T. Solvent effects on the photochemical and fluorescence properties of zinc phthalocyanine derivatives. J Mol Struct 2003; 650:131-140.

[22] Adachi K, Chayama K, Watarai H. Formation of helical J-aggregate of chiral thioether-derivatized phthalocyanine bound by palladium(II) at the toluene/water interface. Langmuir 2006;22:1630-1639.

[23] Isago H. Spectral properties of a novel antimony(III)-phthalocyanine complex that behaves like J-aggregates in non-aqueous media. Chem Commun 2003; (15):1864–1865.

[24] Kaneko Y, Arai T, Tokumaru K, Matsunaga D, Sakurgi H. Observation of novel fluorescent dimer of zinc tetrasulphonatophthalocyanine. Chem Lett 1996;19:345-346.

[25] Saka ET, Gol C, Durmus M, Kantekina H, Bıyıklıo˘glu Z. Photophysical, photochemical and aggregation behavior of novel peripherally tetra-substituted phthalocyanine derivatives. J Photochem Photobiol A Chem 2012;241:67-78.

[26] Adachi K, Watarai H. Interfacial aggregation of thioether-substituted phthalocyaninatomagnesium(II)–palladium(II) complexes in the toluene/water system. J Mater Chem 2005;15:4701-4710.

[27] Dick S, Peisert H, Dini D, Hanack M, Cook MJ, Chambrier I, Chassé T. Influence of the alkyl-chains length on the electronic structure and interface properties of 1,4-octasubstituted zinc phthalocyanines on gold. J Appl Phys 2005;97(7):073715/1-8.

[28] Novakova V, Zimcik P, Kopecky K, Miletin M, Kunesˇ J, Lang K. Self-assembled azaphthalocyanine dimers with higher fluorescence and singlet oxygen quantum yields than the corresponding monomers. Eur J Org Chem 2008;(19):3260–3263.

[29] Adachi K, Chayamab K, Watarai H. Aggregation of thioether-substituted subphthalocyanines with palladium(II) at the toluene–water interface. Soft Matter 2005;1:292–302.

[30] Ma C, Tian D, Hou X, Chang Y, Cong F, Yu H, Du X, Du G. Synthesis and characterization of several soluble tetraphenoxy-substituted copper and zinc phthalocyanines. Synthesis 2005;(5):741–748.

[31] Cong F, Li J, Ma C, Gao J, Duan W, Du X. Tuning J-type dimers of non-peripherally substituted zinc tetra-4-tert-butylphenophthalocyanine. Spectrochimica Acta Part A 2008;71:1397–1401.

[32] Ogunsipe A, Nyokong T. Effects of substituents and solvents on the photochemical properties of zinc phthalocyanine complexes and their protonated

derivatives. J Mol Struct 2004;689(1-2):89-97.

[33] Liu J., Zhao Y., Zhao F., Zhang F., Tang Y., Song X., Effects of Protonation and Deprotonation on Phthalocyanine’s Spectra. Acta phys-chim Sin 1996;12(3):202-207.

[34] Mack J., Stillman M. J., Assignment of the Optical Spectra of Metal Phthalocyanine Anions. Inorg Chem 1997;36:413-425.

[35] Mack J, Stillman MJ. Assignment of the optical spectra of metal phthalocyanines through spectral band deconvolution analysis and ZINDO calculations. Coordin Chem Rev 2001;219-221:993-1032.

[36] Mack J, Stillman MJ. Photochemical formation of the anion radical of zinc phthalocyanine and analysis of the absorption and magnetic circular dichroism spectral data. Assignment of the optical spectrum of [ZnPc(-3)]$^-$, J Am Chem Soc 1994;116:1292-1304.

[37] Mack J, Stillman MJ. Transition assignments in the ultraviolet-visible absorption and magnetic circular dichroism spectra of phthalocyanines. Inorg Chem 2001;40(4):812-814.

[38] Cao Z, Chen Q, Lu Y, Liu Ｈ, Hu Y, Lu Y, Liu H, Hu Y. Electronic absorption spectra of meso-substituted porphyrins and their zinc derivatives. Acta Phy-Chim Sin 2012;28(5):1085-1093.

[39] Zhuang C, Sun Y, Wang Y, Shi J, Shi Y, Shi T. Preparation and properties of 5-(4-nicotinicaminophenyl)-10,15,20- triphenylporphyrin and its Zn complexes, Acta Chim Sin 2010;68(22):2319-2324.

[40] Nombona N, Chidawanyika W, Nyokong T. Spectroscopic and physicochemical behavior of magnesium phthalocyanine derivatives mono-substituted with a carboxylic acid group. J Mol Struct 2012;1012:31-36.

[41] Lin MJ, Fang X, Xu MB, Wang JD. The effect of protonation on the spectra and stabilities of alkoxyl substituted phthalocyaninatometals. Spectrochim Acta A 2008;71:1188–1192.

[42] Nakai K, Usami J, Kobayashi N. Metal phthalocyanine showing four-peak Q-band similar to metal-free phthalocyanines: nickel 1,4-di(trifluorosulfonyl)-phthalocyanine. J Porphyrins Phthalocyanines 2007;11:222-227.

[43] Cong F, Ning B, Ji Y, Wang X, Ke F, Liu Y, Cui X., Chen B., The facile synthesis and characterization of tetraimido-substituted zinc phthalocyanines. Dyes Pigments 2008;77:686-690.

[44] Cong FD, Ning B, Yu HF, Cui XJ, Chen B, Cao SG, Ma CY. The control of phthalocyanine properties through nitro-group electronic effect, Spectrochim. Acta A 2005;62:394-397.

[45] Furuyama T, Satoh K, Kushiya T, Kobayashi N. Design, synthesis, and properties of phthalocyanine complexes with main-group elements showing main absorption and fluorescence beyond 1000 nm. J Am Chem Soc 2014;136:765-776.

[46] Cong FD, Ning B, Du XG, Ma CY, Yu HF, Chen B. Facile synthesis, characterization and property comparisons of tetraaminometallophthylocyanines with and without intramolecular hydrogen bonds. Dyes Pigments 2005;66:149-154.

[47] Novakova V, Miletin M, Kopecky K, Zimcik P. Red-Emitting dyes with photophysical and photochemical properties controlled by pH. Chem Eur J 2011; 17:14273-14282.

[48] Makhseed S, Tuhl A, Samuel J, Zimcik P, Al-Awadi N, Novakova V. New

highly soluble phenoxy-substituted phthalocyanine and azaphthalocyanine derivatives: Synthesis, photochemical and photophysical studies and atypical aggregation behavior. Dyes Pigments 2012;95:351-357.

[49] Cong FD, Wang HF, Li JX, Li LL, Yan QY, Chu XX, Meng YY, Xing KZ, Du XG. Improved synthesis and chromophoric properties of tetra-b-(2-octanyloxy)substituted nickel phthalocyanine. Asian J Chem 2014;26:2351-2356.

[50] Vior MCG, Dicelio LE, Awruch J. Synthesis and properties of phthalocyanine zinc(II) complexes replaced with oxygen and sulfur linked adamantane moieties. Dyes Pigments 2009:83:375-380.

[51] Tian J, Jing L, Zhang C, Ji L, Zhu P, Zhang X. Helical self-assembly of optically active phthalocyanine derivatives bearing four optically active (S)-2-methylbutoxy moieties at the α position of the phthalocyanine ring. Eur J Inorg Chem 2013;2013(30):5281-5287

Captions of Figures and Scheme

Fig. 1 Mass spectrum of *α*OZnP: m/z, 1089.8 for monomer.

Fig. 2 UV-vis spectra of solutions (2.0×10^{-5}, 5.0×10^{-6} and 1.25×10^{-6} mol/L, *α*OZnP in chloroform) (a), (1.0×10^{-5} mol/L, *α*OZnP in chloroform with acetic acid from 0 to 2.68×10^{-1} mol/L) (b), (1.0×10^{-5} mol/L, *β*OZnP in chloroform after adding 0, 1, 2 and 3 droplets of acetic acid, and 5 droplets of triethylamine in order) (c), (1.0×10^{-5} mol/L, *α*OZnP in chloroform with triethylamine from 0 to 6.59×10^{-3} mol/L) (d).

Fig. 3 Schematic representation of proposed *α*OZnP and (*α*OZnP)H^+ in chloroform.

Fig. 4 UV-vis spectra of solution (1.0×10^{-5} mol/L, *α*OZnP in benzene with triethylamine from 0 to 6.59×10^{-3} mol/L) (a), and (1.0×10^{-5} mol/L, *α*OZnP in THF with acetic acid from 0 to 50 droplets.) (b).

Fig. 5 UV-vis spectra of solution (1.0×10^{-5} mol/L, *α*OCuP in chloroform with acetic acid from 0 to 40 droplets) (a), and (1.0×10^{-5} mol/L, *α*OCuP in benzene with acetic acid from 0 to 20 droplets) (b).

Fig. 6 UV-vis spectra of the detection solutions (c_0, *α*OZnP in chloroform with various concentration of acetic acid from c_1 to c_8) with respect to the initial solution (c_0, *α*OZnP in chloroform without acetic acid) (a); and the linear relationship between the concentration logarithm of acetic acid in chloroform (lg c) from c_3 to c_7 and the relative difference value of altered absorbance (⊿A) at around 752 nm and 706 nm, respectively (b).

Scheme 1 Synthesis and molecular structures of *α*OZnP, *α*OCuP and *β*OZnP.

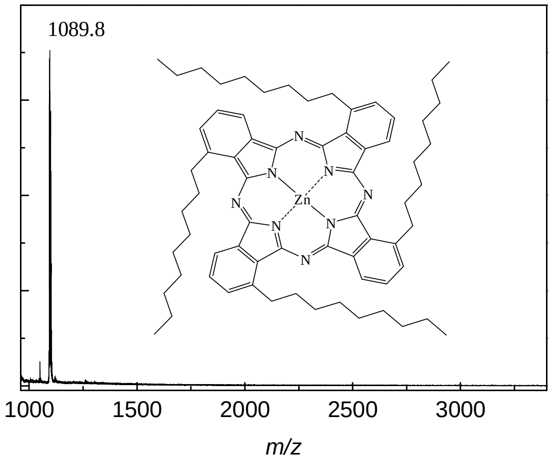
1089.8
N
Zn
1000
1500
2000
2500
3000
m/z

Fig. 1

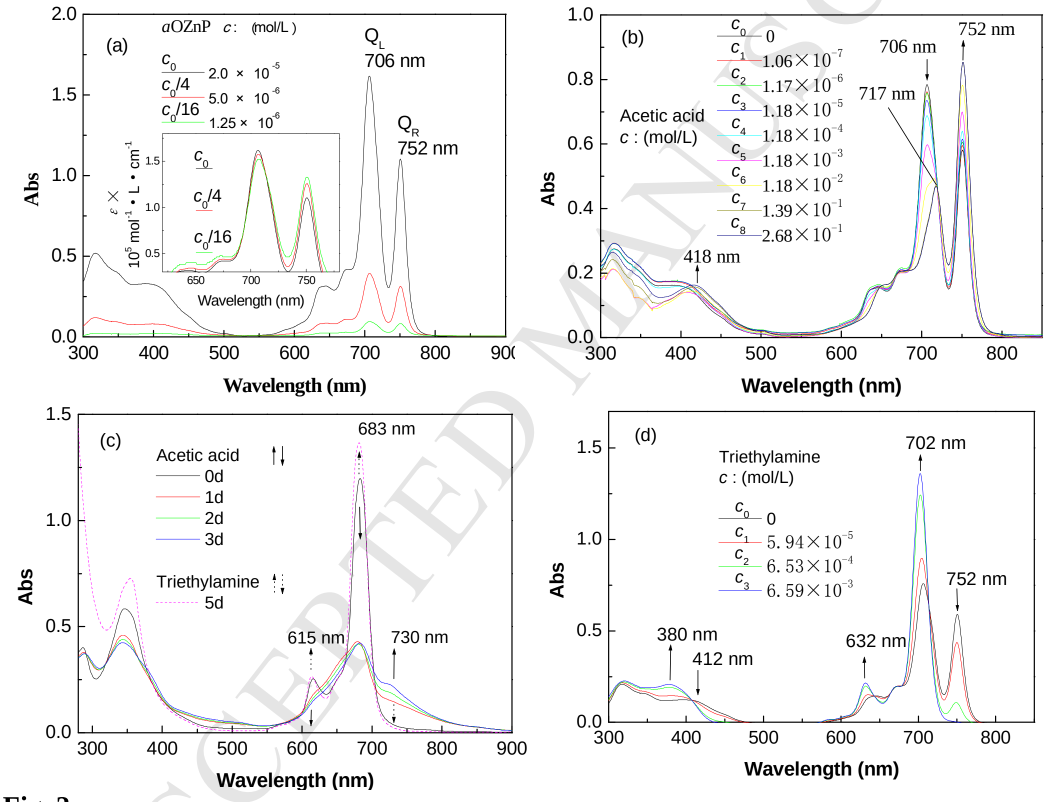
(a)
aOZnP c : (mol/L)
c0 2.0 × 10-5
c0/4 5.0 × 10-6
c0/16 1.25 × 10-6
QL
706 nm
QR
752 nm
ε × 10^5 mol^-1 • L • cm^-1
Wavelength (nm)
Abs
Wavelength (nm)
(b)
Acetic acid
c : (mol/L)
c0 0
c1 1.06×10^-7
c2 1.17×10^-6
c3 1.18×10^-5
c4 1.18×10^-4
c5 1.18×10^-3
c6 1.18×10^-2
c7 1.39×10^-1
c8 2.68×10^-1
706 nm
752 nm
717 nm
418 nm
Abs
Wavelength (nm)
(c)
Acetic acid
0d
1d
2d
3d
Triethylamine
5d
683 nm
615 nm
730 nm
Abs
Wavelength (nm)
(d)
Triethylamine
c : (mol/L)
c0 0
c1 5.94×10^-5
c2 6.53×10^-4
c3 6.59×10^-3
702 nm
752 nm
380 nm
412 nm
632 nm
Abs
Wavelength (nm)

Fig. 2

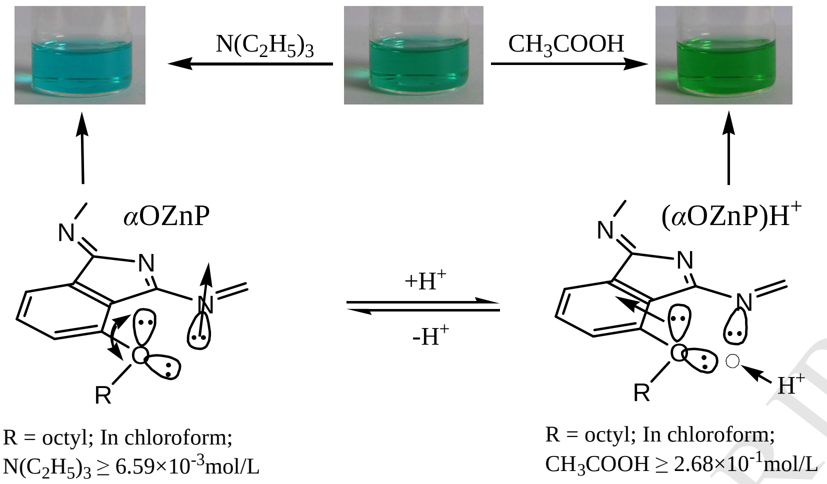

Fig. 3

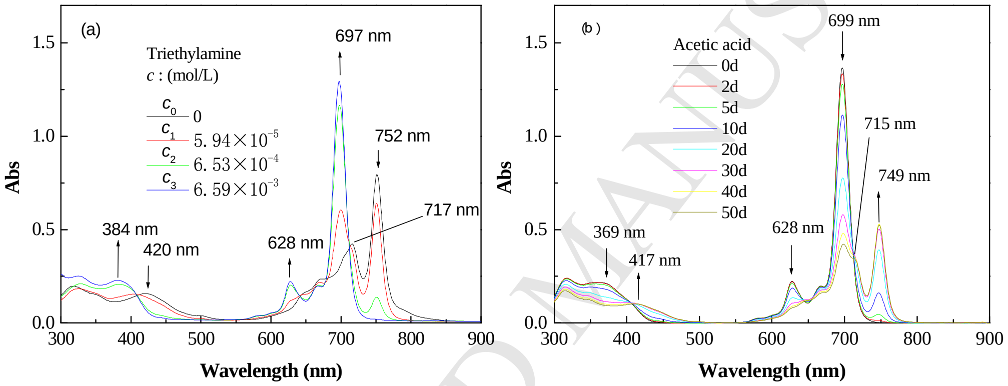

Fig. 4

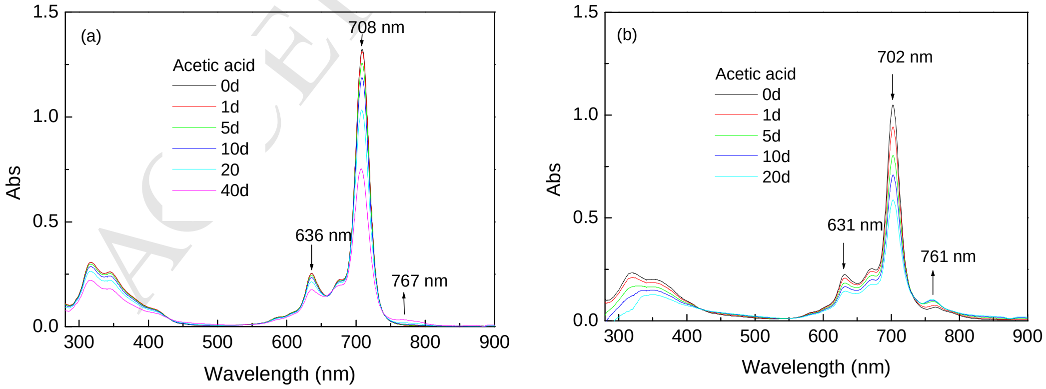

Fig. 5

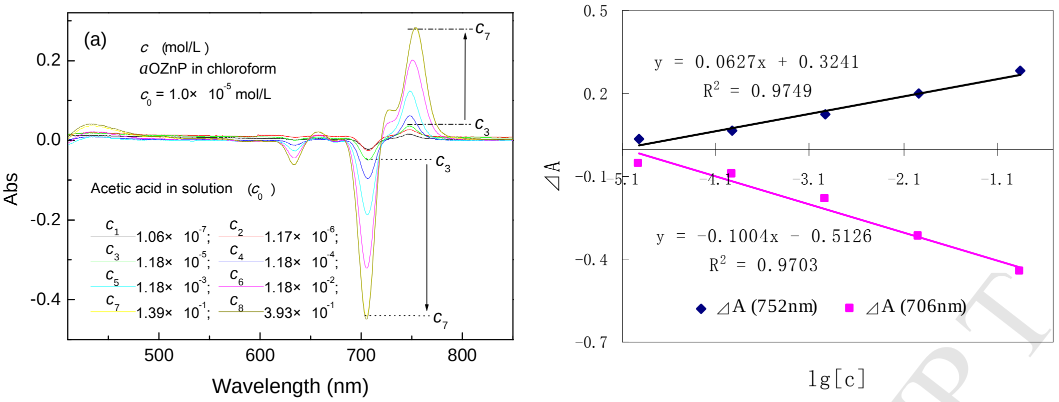

Fig. 6

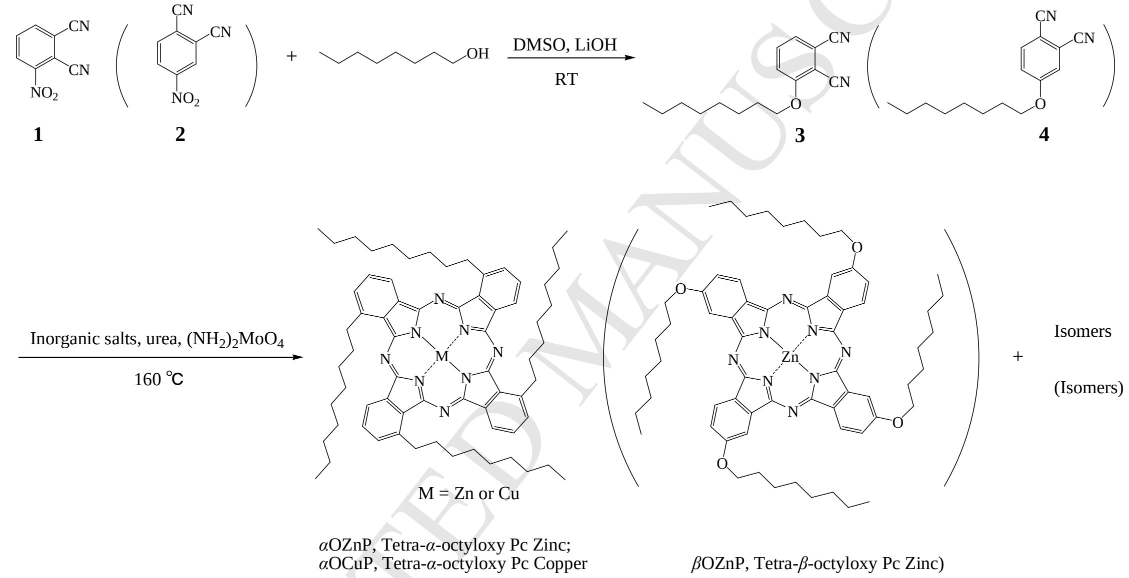

Scheme 1

Characteristic absorption band split of symmetrically tetra-octyloxy metal phthalocyanines

- ► Symmetrically substituted metal phthalocyanines behave Q band split;
- ► The split requires zinc, α-substituted position and non-coordinated solvent;
- ► The split peaks could be tuned by acid and alkali as well as solvents;
- ► The altered Q absorbance is linear with the concentration logarithm of acid.